STAT

Next 3 Page(s) In Document Denied

Engineering Services on

TRANSISTORS

SEVENTH INTERIM TECHNICAL REPORT

Covering the Period 16 September to 15 December 1956

Signal Corps Contract DA 36-039 sc-64618

Signal Corps Project No. 323A

Department of the Army Project No. 3-19-03-031

This contract is a joint services contract for the Departments of the Army, Navy, and Air Force. It calls for services, facilities, and materials to be employed in studies and investigations related to transistors and transistor-like devices, together with their circuit properties and their applications for military uses.

This report was prepared by Bell Telephone Laboratories Incorporated
The following engineers and scientists participated in its preparation:

W. L. Brown J. E. Iwersen C. H. Knowles J. T. Nelson J. Sevick

SUMMARY OF STATUS

As reported in Sections 2 and 3, Tasks 1, 3, and 6 have been completed. No work was done on Task 7 during this report interval. Task 8 is covered in a separate series of reports. Work done on the other tasks is summarized below.

During the period covered by this report, 16 September through 15 December 1958, approximately 5 000 hours were devoted by key personnel to work on this project.

TASK 2 - TRANSISTOR RELIABILITY

On account of the heavy demand for aging information from users of transistors, the direct determination of reliability is still being pushed, especially for the newer transistors. Tests on time rates of aging of particular transistors with temperature and with applied voltage are under way and a preliminary report may be available next quarter. Although the results of this type of test are dependent on changes and improvements in fabrication, it is believed that the greater stability now available from new surface processing and the need for information on new types make this work of continuing urgency.

Correlation of the observed aging trends with the physical causes is continuing, under difficulties caused by the inherent sensitivity of the surfaces to contamination by atomic amounts of water, oxygen, and other trace ambients. An experiment to study simultaneously surface properties and aging of junction characteristics in the same ambient has been undertaken, from which it is hoped to separate the physical causes and thereby improve the understanding and effectiveness of the aging measurements.

TASK 4 - NEW AND IMPROVED TRANSMISSION-TYPE TRANSISTORS

Development of diffused-base germanium and silicon transistors has continued. Temperature studies of characteristics and performance have been made on the M2039 diffused-base germanium p-n-p oscillator transistor under Industrial Preparedness Study Contract DA 36-039 sc-72729. Excellent oscillator efficiencies were obtained, even at 100°C. Development activity on the M2055 and M2058 low-level common-base and common-emitter amplifier designs has been expanded under the same contract. The characteristics of initial models of these diffused-base germanium devices are also very encouraging.

Modifications in the structure of the M2036 p-n-i-p silicon power transistor have increased the oscillator efficiency of this device so that efficiencies above 50 per cent and powers greater than 5 watts have been obtained in experimental units at 10 mc. Oscillator performance testing has been accompanied by other characterization work such as d-c, low-frequency, and high-frequency parameter measurements. These results have been compared with a proposed equivalent circuit and with pulse-measurement data. The initial design objectives for this unit have been reached.

TASK 5 - TRANSISTOR TEST METHODS

Chapter 6 describes the present status of the 5-mc to 250-mc Phase Set and discusses improved crosstalk performance, signal to noise ratio, and improvements in the synchronization system performance.

TABLE OF CONTENTS

LIST OF ILLUSTRATIONS

SECTION 1 - PURPOSE

The general purpose of this contract is to make studies and investigations related to transistors and transistor-like devices, together with their circuit properties and applications, with a view toward demonstrating and increasing the practicality of their use in operating equipment. This contract is a successor to two preceding contracts of a similar nature: Contract W36-039 sc-44497, herein after referred to as the First Engineering Services Contract on Transistors; and Contract DA 36-039 sc-5589, hereinafter referred to as the Second Engineering Services Contract on Transistors. Both of these contracts were included in Department of the Army Project 3-19-03-031 and Signal Corps Project 27-323A-1. The reports on these contracts contain much reference material, particularly on dual-stability switching circuits suitable for data transmission and also on other properties of various transistors and related devices. Unless otherwise stated, all references to previous reports are to those produced under this, the Third Engineering Services Contract.

These contracts call for services, facilities, and material to be employed on mutually acceptable tasks. Of the eight tasks assigned, three have been completed. Task 1 involved the development of an oscillator of very low power drain, the Final Report on this task was issued on 1 June 1952. Task 3 covered a symposium on the circuit properties of transistors; the Final Report on this task was issued on 1 February 1952. Task 6 called for theoretical and experimental studies leading to the development of photocell blocks as set forth in the specifications for p-n junction photocells and photocell blocks (NRL Problem R05.54); the Final Report on this task was issued on 31 January 1955.

The other assigned tasks are outlined below. Although Task 8 is being covered by separate reports, an outline of this task as agreed to between the contracting parties is also included here.

The terms "zero-order exploratory development" and "first-order feasibility development" employed in the following outlines are defined in two reports issued under the First Engineering Services Contract on Transistors: the Sixth Quarterly Report, pages 11 to 13, and the Final Report, Section 4, pages 5 and 6.

TASK 2 - TRANSISTOR RELIABILITY

The contractor shall conduct a broad program in transistor reliability designed to accomplish the following objectives:

(a) Provide quantitative definitions of transistor and transistor circuit reliability figures of merit.

(b) Evaluate available transistors in the light of the above definitions.

(c) Explore the possibilities of developing more reliable transistors in terms of (a) above.

TASK 4 - NEW AND IMPROVED TRANSMISSION-TYPE TRANSISTORS

The contractor shall make theoretical and experimental studies leading to zero-order exploratory development and, upon mutual agreement, to first-order feasibility development of:

(a) New transistors using new or previously untried principles.

(b) New transistors obtained by studied modifications of existing types.

The new transistors shall be primarily intended and suitable for application to voltage, current, and power amplifiers, and associated electronic transducers. In particular, it is desirable to carry through the zero- and first-order development of a point-junction transistor for micropower radio-frequency applications.

In general, a-c amplifying devices for voltage, current, and power amplification, which are of particular interest, have transmission properties in the following ranges:

(a) Frequency range: two cycles per second to 100 megacycles; this range need not be achieved in one transistor.

(b) Voltage ranges: one microvolt to fifty volts; same comment.

(c) Current ranges: one microampere to one ampere; same comment.

(d) Power ranges: one microwatt to ten watts; same comment.

(e) Noise figures at 100 cycles per second; two decibels as a goal.

Class A and AB operation is intended. Per cent harmonic distortion is indicated at three per cent as a goal. In order to arrive at useful devices it will be necessary to keep in mind the eventual importance of simplicity of operation and construction, interchangeability of transistor units, drifts of important circuit parameters, such as gain, selectivity, distortion, etc., with time, temperature, and climatic conditions, in that order of importance. Avoidance of unusual circuit requirements, such as inordinately low per cent regulation in power supplies or cumbersome associated equipment is also an ultimate desideratum.

For CW oscillator service, device properties in the following ranges are of particular interest:

(a) Frequency range: twenty cycles per second to 100 megacycles, not necessarily in one unit.

(b) Power ranges: ten microwatts to five watts.

(c) Frequency stability: Variations of device characteristics which affect frequency should be comparable to those of electron tubes commonly used in electron-coupled oscillators.

The transistors to be ultimately developed for manufacture are intended to improve the electronic contrivances now available using electron tubes in the matter of:

(a) Operating parameters, such as gain, selectivity, noise, drift, operating life;

(b) Physical size and weight (reduction);

(c) Power requirements (reduction);

(d) Cost;

(e) Simplicity of construction and operation;

(f) Maintenance problems;

(g) Effect of extraneous environmental influences, such as temperature, humidity, shock and bounce, and pressure.

TASK 5 - TRANSISTOR TEST METHODS

Task 5 involves the formulation of requirements for transistor test equipment and the fabrication of an experimental model.

TASK 7 - TRANSISTOR CIRCUIT COMPONENTS

Task 7 specifies studies and investigations of suitable miniaturized components for transistor circuit applications aimed toward the following four major objectives:

(a) To determine appropriate electrical ratings and the most suitable mechanical characteristics for component apparatus such as inductors, transformers, capacitors, resistors, potentiometers, power supplies, etc., presently needed in transistor circuitry.

(b) To determine what types of components meeting these requirements are currently available in reasonably satisfactory form.

(c) To report on the status of work being carried on at Bell Telephone Laboratories on the development of miniaturized components to meet the stated requirements.

(d) To formulate recommendations as to areas of component development work not being adequately covered by Bell Telephone Laboratories and on which the military services might concentrate fruitful additional development and research effort elsewhere.

TASK 8 - IMPROVED CRYSTAL RECTIFIERS

The contractor shall make theoretical and experimental studies leading to zero-order exploratory development, and upon mutual agreement, to first-order feasibility development and to second-order development of:

(a) New crystal rectifiers using new or previously untried principles.

(b) New crystal rectifiers obtained by studied modifications of existing principles.

The new crystal rectifiers shall be primarily intended and suitable for application to broadband microwave mixers.

Since Task 8 is being supported solely by the Signal Corps Procurement Agency, and is of interest in a separate group of applications, it is being issued as a separate report under Contract DA 36-039 sc-5589.

The zero-order research and exploratory development shall be carried on in three phases:

(a) The development of a comprehensive design theory of the crystal rectifier by extension of the p-n theory of rectifiers to the required frequencies and signal levels shall be carried on in the first phase. The theory should relate the large- and small-signal impedances to the resulting conversion characteristics. Moreover, it should relate the large- and small-signal impedances, the noise, and the power capabilities to the material and structural properties of the device.

(b) The second phase shall include the exploration and evaluation of materials and techniques. Examples of materials might be silicon, germanium, silicon-germanium alloys, or the intermetallic compounds. Examples of techniques might be diffusion, alloying, remelting, or bombardment.

(c) The third phase shall include the fabrication of exploratory crystal rectifiers and a determination of their characteristics to check the zero-order theory.

Upon mutual agreement the Task may include first-order feasibility development which shall be carried on in the following manner:

(a) The first phase shall involve a refining of the zero-order theory in light of the findings of (c) above. The theory shall be extended to include a study of reliability factors, such as temperature, humidity, shock, and vibration.

(b) The second phase shall constitute a choice of material and technology.

(c) In the third phase sufficient crystal rectifiers shall be fabricated to determine feasibility.

The performance objectives to be sought by these designs shall be:

(a) Improvements in the order of two to three db for conversion loss and a two-to-one reduction in noise ratio over present-day crystal rectifiers.

(b) Crystal rectifiers capable of operating over a 12 per cent bandwidth.

(c) Crystal rectifiers having substantial improvement in regard to burn-out by high level pulses.

(d) Balanced crystal rectifiers and reversed polarity crystal rectifiers shall be investigated.

Upon mutual agreement, the Task may include second-order development, based on the information gathered in the zero-order and first-order development, applied to the design of one or more specific crystal rectifers. These crystal rectifiers would be specific in the sense that they would be designed to operate at a fixed-frequency range and bandwidth between specific impedance levels and under specific power levels. Particular attention would be given to the reproducibility and reliability of the crystal rectifier. No development of the mixer plumbing would be anticipated.

The specific development would lead to the gathering and writing of second-order design information and the supplying of 200 sample models.

SECTION 2 - ABSTRACT

TASK 2 - TRANSISTOR RELIABILITY

This report contains two chapters: one on neutron radiation damage to certain transistors and diodes, and one in an attempt to correlate aging behavior with noise measurements. Although neither of these studies was made on the subject contract, they are reported because they are closely related to the field of Task 2.

A preliminary study of the neutron radiation sensitivity of five types of germanium transistors and five types of silicon diodes is reported in Chapter 1. All measurements were performed outside the neutron environment several weeks after the neutron exposure. The extent to which the various devices were affected varied enormously. Changes in resistivity, junction capacity, and lifetime (as manifested by change in alpha for the transistors and change in forward current for the diodes) can be reasonably well explained by the expected radiation damage changes in the bulk properties. The universally observed increase in reverse junction current cannot similarly be explained and apparently results from degradation in the device surfaces.

In Chapter 2, noise measurements are reported that were made on silicon diodes in an attempt to correlate these measurements with aging behavior in a short test. If sucessful, the correlation would be an important aid in quick prediction of reliability. Although no correlation was found, it is still believed that physical mechanisms producing aging trends must be related to those producing noise; consequently, a correlation should appear some day when the phenomena are more completely analyzed.

TASK 4 - NEW AND IMPROVED TRANSMISSION-TYPE TRANSISTORS

The work on development of transmission transistors is reported in three chapters. Results on germarium diffused-base transistors are to be found in Chapters 3 and 4, which give, respectively, oscillator performance and parameter measurements on the M2039 at 100°C and preliminary results on the low-level amplifiers M2055 and M2058.* The preliminary studies of the P-N-I-P Silicon power transistor (M2036) are in Chapter 3.

The high-temperature studies on the M2039 in Chapter 3 show that oscillator efficiencies at 200 mc decrease from 44 per cent to 32 per cent as temperature is increased from 26°C to 100°C. Parameter measurements also reported in Chapter 3 show that collector reverse current increases to about 150 microamperes as temperature increases to 100°C. The 100-mc common-emitter current gain decreases about 1 to 2 db in the same temperature rise. Ohmic base resistance is substantially

*Although this work is being done under Industrial Preparedness Study Contract DA 36-039 sc-62929, it is reported here because of its bearing on future work of the Development Contract

unaffected by the temperature increase. Low-frequency h-parameters vary in approximately the manner expected from theory.

A number of low-level germanium diffused-base amplifiers have been made, as reported in Chapter 4. The mechanical design of the M2055 common-base low-level r-f amplifier unit and the M2058 common-emitter broadband unit has been modified to simplify fabrication and improve reliability. These changes have permitted the fabrication of about sixty units with very encouraging electrical characteristics. Of these units, 60 per cent had common-emitter short-circuit current gains (β) at 100 mc in excess of 12 db, and 33 per cent have gain greater than 14 db. Low-frequency $1 + h_{21}$ is unsatisfactorily high at present, with a center around 0.05. Work on all three of these diffused-base germanium types will continue under the Industrial Preparedness Study Contract.

Laboratory models of the M2036 p-n-i-p power transistor are described in Chapter 5. The structure has been modified by reduction of the collector area and of the base-to-emitter spacing, and the base region has also been made thinner. These changes have produced wafers which deliver more than 5 watts r-f output power at 10 mc. Characterization studies have shown alpha cutoff frequencies in the 60- to 90-mc range as extrapolated from common-emitter measurements. A simple equivalent circuit for this device has been proposed and approximately verified by radio-frequency bridge measurements. Comparison of pulse and small-signal measurements indicate discrepancies possibly associated with collector series resistance or with nonlinearities in the device. The high-power performance capability of the M2036 design has been demonstrated. Continuation of this development is planned.

TASK 5 - TRANSISTOR TEST METHODS

Chapter 6 describes the present status of the 5-mc to 250-mc Transistor Phase Set. The following items are discussed:

(1) Improved crosstalk performance in the measuring path switches

(2) Signal-to-noise ratio data on the amplifier-modulator

(3) Improvements in the synchronization system performance

SECTION 3 - PUBLICATIONS AND REPORTS

No publications or reports were issued during this period.

SECTION 4 - FACTUAL DATA

TASK 2 - TRANSISTOR RELIABILITY

Chapter 1

NEUTRON RADIATION EFFECTS ON GERMANIUM TRANSISTORS AND SILICON DIODES

By W. L. Brown

1.1 INTRODUCTION

In the interests of exploring the sensitivity of semiconductor devices to a neutron environment, a group of germanium transistors and silicon diodes were irradiated in the Brookhaven National Laboratories nuclear reactor. In addition to the author, a large number of people contributed assistance and stimulation to the work. Their contributions are gratefully acknowledged.

Pile radiation produces effects on semiconductor devices in several different ways:

(1) Through transmutations of the semiconductor atoms to chemical donor and acceptor atoms

(2) Through displacements in the atoms of the lattice (bombardment damage), the vacancies and interstitials thus produced acting like donors, acceptors, and recombination centers

(3) Through ionization in the lattice, which gives hole-electron pairs in much the same way that light does

(4) Through surface effects, either by direct interaction of the radiation with the semiconductor surface or through interaction with the encapsulating container or its filling medium

The rate of generation of hole-electron pairs is approximately $g = 2 \times 10^{10} R/cm^3 sec$ where R is the radiation field in roentgen per hour. With a life time τ and diffusion constant D this results in a junction current $i_j = 3 \times 10^{-9} R \sqrt{D\tau}$ amp/cm^3 which for a lifetime in germanium on the order of ten microseconds is a current $i_j = 1 \times 10^{-10} R$ amp/cm^2. None of the measurements to be described here were made in the pile, so that ionization occurs only as a result of the radioactivity of the units following the neutron radiation. By the time the units were measured, R was much less than 1 r/hr, so that the current developed in this way was negligible. In the pile, where the radiation field may be 10^6 r/hr, the added junction current might be quite important.

With the usual spectrum of pile neutrons, and with temperatures sufficiently low (less than about 200°C), so that a substantial part of the bombardment damage has not annealed, the effect of transmutations is generally small compared with the effect of bombardment damage.

The present experiments are thus concerned with body effects of radiation damage, about which considerable is known and more can be reasonably estimated, and with surface effects, about which essentially nothing is known. We will attempt to assess to what extent one or the other of these is dominant.

1.2 THE DEVICES AND THEIR NEUTRON EXPOSURES

Five types of germanium transistors were irradiated with integrated thermal neutron fluxes of 10^{13}, 10^{14}, and 10^{15} neutrons/cm^2. Two 1893 point-contact units, two 1868 p-n-p alloy units, two 1853 n-p-n alloy units, two 1859 n-p-n grown-junction units, and one 1777 p-n-p alloy unit were subjected to each of the three neutron doses.

Five types of silicon diodes were given exposures of 10^{15} and 10^{16} n/cm^2. Two 2048 and two 2032 double-diode voltage regulator units, two 2025 and two 2029 power-diode units, and two solar batteries were each given the two neutrons doses.

The flux level of the exposures was about 2.5 x 10^{12} thermal neutrons/cm^{2}sec. Radiation damage is produced by the fast neutron flux, which is roughly 30 per cent as large. In the remainder of this report, the flux figures given represent the integrated thermal flux as provided by Brookhaven National Laboratories. The temperature during radiation was less than 60°C, and probably less than 50°C, in all cases.

Nuclear reactions in the semiconductors and their leads and encapsulating envelopes made the units highly radioactive, particularly in the devices given larger integrated fluxes and involving massive pieces of copper for cooling purposes. No electrical measurements were made on the units until several weeks after the neutron exposures, to allow the radioactivity to decay to a safe level. Even short of studying the devices during actual radiation, there is a large time interval which has not been explored in the present experiments and in which there might be ionization-induced junction currents and perhaps important effects of readjustment in surface chemistry.

1.3 INTERPRETATION OF CHANGES IN DEVICE CHARACTERISTICS

In this section the various types of devices are discussed individually. A large number of parameters were measured for some types and only a few for others. Particular attention has been paid to changes in reverse current, alpha, and junction capacity for the transistors, and in reverse current, forward current, and capacity for the diodes.

1.3.1 1893 Germanium Point-Contact Transistors

At exposures of 10^{13} and 10^{14} n/cm^2 the characteristics of these units were practically unchanged. At 10^{15} n/cm^2 the collector current at zero emitter current rose by a large factor, and the devices lost transistor action. These units are made of four- to six-ohm cm n-type germanium (donor concentration ≈ 4 x 10^{14}/cc). Radiation damage by neutrons, according to Cleland, Crawford, and Pigg* introduces net acceptors in n-type material at a rate ≈ 2 acceptors/cm^3/neutron/cm^2 (two acceptors/neutron cm). Consequently one would expect the n-type material to convert to p-type between 10^{14} and 10^{15} n/cm^2. The observed changes bear out this expectation. Surface effects in these units seem to play no important role.

*Cleland, Crawford, and Pigg, Physical Review, Vol. 98, 1955, p. 1742.

1.3.2 1868 P-N-P Germanium Alloy Transistors

At 10^{13} and 10^{14} n/cm^2 these devices suffered a progressive increase in reverse collector current, a progressive decrease in alpha, and, at 10^{14} n/cm^2, a measurable decrease in collector capacity. At 10^{15} n/cm^2 the units failed, essentially with shorts between emitter and collector. The decrease in collector capacity at 10^{14} n/cm^2 indicates the introduction of acceptor centers at a rate approximately two per neutron cm. The failure at 10^{15} n/cm^2, as in the preceding case, can be attributed to conversion of the base material from n- to p-type. If the changes in alpha (which before radiation was about 0.95) are interpreted as merely due to a decrease in electron lifetime in the base region, assumed to be 1-mil thick, at 10^{14} n/cm^2 $\tau \approx 1$ microsecond. The lifetime due to radiation damage at 10^{13} n/cm^2 (the change in net lifetime is so small the result lacks accuracy) is about ten microseconds, agreeing with the notion that bombardment introduces recombination centers at a constant rate. There are no measurements available of bulk lifetime change produced by neutron radiation, but one can make a judicious, if somewhat unreliable estimate by analogy with experiments of lifetime degradation by electron radation damage carried out by Loferski and Rappaport* in n-type germanium. Using the rate of change of conductivity by electrons and by neutrons as a means of comparing their effectiveness in introducing damage, and assuming the same ratio applies to degradation of lifetime, one calculates a lifetime of about 0.3 microsecond for 10^{14} n/cm^2. The agreement is at least as good as could be expected, and makes it plausable that the alpha degradation does result from body-lifetime change.

Using the value for the lifetime obtained from alpha (the change in base resistivity is too small to be considered) one can calculate the change in I_{co} to be expected due to change in hole current flowing across the collector junction. At 10^{14} n/cm^2 the increase should be about 3 microamperes, about an order of magnitude less than observed. This it seems that while capacity and alpha changes are consistant with expected changes in body properties of the base material, the change in collector current is dominated by some surface effect, details unknown. Clearly one would like to re-etch the radiated units to check this point. Such measurements have not yet been made.

Table 1-1

Changes in 1868 P-N-P Units

n/cm²	Parameter Measured		
	ΔI_{co}	Alpha	ΔC_c
10^{13}	$\approx 5\mu a$	0.91	$<1\mu\mu f$
10^{14}	$\approx 25\mu a$	0.80	$-2\mu\mu f$
10^{15}	—	—	—

Table 1-2

Changes in 1853 N-P-N Units

n/cm²	Parameter Measured		
	ΔI_{co}	Alpha	ΔC_c
10^{13}	$1.5\mu a$	0.98	$<1\mu\mu f$
10^{14}	$14\mu a$	0.975	$+1\mu\mu f$
10^{15}	$120\mu a$	0.71	$+5\mu\mu f$

*Loferski and Rappaport, Physical Review, Vol. 98, 1955, p. 1861.

1.3.3 1853 N-P-N Germanium-Alloy Transistors

These devices showed progressive increases in I_{co}, decreases in alpha, and increases in collector capacity throughout the range of radiation.

Since the radiation introduces acceptors in the p-type base, one does not expect failure with emitter to collector shorts. The increase in capacity indicates this increase in acceptor concentration and gives a value of about 0.5 acceptor neutron cm which compares quite reasonably with the value of 0.7 given by Cleland, Crawford, and Pigg* for p-type germanium. Attributing the change in alpha to change in base lifetime, as for the 1868, one finds a bombardment-induced lifetime of 50 microseconds, 8 microseconds, and 0.3 microsecond for the three neutron doses. This is only very crudely inversely proportional to bombardment. Note that the lifetime in p-type is degraded less rapidly by bombardment than in n-type. No measurements of bulk properties are available to check this point. Again, using the lifetime deduced from alpha to calculate an increase in I_{co} one obtains values about an order of magnitude less than the measured increases. The surface again seems to play a dominant role in the junction currents.

1.3.4 1859 N-P-N Germanium Grown-Junction Transistors

Unfortunately no prebombardment measurements are available for these units. Alpha is significantly smaller and I_{co} significantly larger for units with a large radiation dose, much as in the alloy n-p-n transistors, but quantitatively little can be said.

1.3.5 1777 P-N-P Germanium Alloy Power Transistors

Even at the 10^{13} n/cm^2 level these units suffered very badly. The collector current became the order of a milliampere compared with 50 to 100 microamperes before radiation, and varied in no systematic way between the 10^{13} and 10^{15} n/cm^2 samples. Even taking into account the larger area of the 1777 (a factor of about 25) the change in I_{co} is an order of magnitude larger than in the 1868 at 10^{13} n/cm^2. No alpha measurements could be made with these units so enormous were the currents. Something in the surface treatment or the encapsulating can (the filling medium in both 1777 and 1868 is dry air) must be very significantly different to account for the different sensitivities of the two devices to neutrons.

1.3.6 2032 and 2048 Double-Diode Silicon Voltage Regulators

Even at exposures of 10^{16} n/cm^2 these devices survived with only minor changes. The breakdown voltages of the units were between 11 and 20 volts, completely unchanged by radiation. The base p-type material was between 0.01 and 0.06 ohm cm, and the acceptor concentration the order of 10^{17} -10^{18}/cm^3. Up to neutron doses the order of 10^{17} n/cm^2, one would not expect to find an important change in base resistivity or, correspondingly, in breakdown voltage. There were significant but not consistant increases in reverse current among these units, but never to an extent to place the units outside their device specifications. The larger device, the 2032, has a heavy copper mounting screw, for heat dissipation, and showed high radioactivity for weeks after bombardment.

*Cleland, Crawford, and Pigg Physical Review, Vol. 99, 1955, p. 1170.

1.3.7 2025 and 2029 Silicon Power Diodes

These diodes depend for their extremely low forward resistance upon conductivity modulation of the nominally 50-ohm cm p-type base material. This modulation requires a base lifetime the order of 10^{-7} seconds, with base layers about 1-mil thick. Even after 10^{15} n/cm^2 the lifetime was apparently less than this, and the forward characteristic was limited by the resistance of the base. The base resistivity deduced from the forward characteristic was about 100 ohm cm after 10^{15} n/cm^2, and between 10^5 and 10^6 ohm cm with 10^{16} n/cm^2. This is in accord with the expectation that, in p-type silicon, bombardment introduces net donor centers in such a way as to make the resistivity approach intrinsic. (Both n- and p-type silicon increase in resistivity with radiation; no evidence of a conversion in type has been seen.) The junction capacity showed a decrease at 10^{15} n/cm^2, and a further decrease to a value too small to be measured reliably at 10^{16} n/cm^2, in agreement with the resistivity figures. The consistency of these two types of measurement shows there is no large change in carrier mobility produced by the bombardment. There were increases in reverse current which correlated roughly with bombardment, but which showed considerable scatter. These increases, even in the large 2025 device at 10^{16} n/cm^2, were no larger than 50 microamperes at 200 volts.

A crude lifetime estimate of 5×10^{-9} seconds with 10^{15} n/cm^2 can be made, based as in the germanium cases on measurements with electron bombardment. This value is certainly consistant with disappearance of the conductivity modulation under forward bias. It does not explain the reverse currents, which in the simple calculation would require a lifetime the order of 10^{-17} second. Probably the reverse currents again arise from some surface condition.

1.3.8 Solar Batteries

The solar cells lost efficiency quite drastically at 10^{15} n/cm^2, and even more at 10^{16} n/cm^2. Both open-circuit voltage and short-circuit current dropped with standard illumination. There are several possible effects which may be contributing.

(1) Carriers produced by light near the surface may not be able to get through the p-type diffused surface layer to the junction in their lifetime. This required $\tau_n < 2 \times 10^{-9}$ seconds, a figure the same order as expected for 10^{15} n/cm^2. This process must at least be important.

(2) The junction may have high saturation current because of low lifetime in the n-type base material. This requires $\tau_p < 10^{-11}$ seconds.

(3) The junction may be shorted by some spurious conducting path.

D. A. Kleinman has pointed out that with the presence of boron, which has a very large neutron capture cross section, the bombardment damage situation may be complicated. In the solar battery the diffused layer is boron, the concentration of boron at the surface of the layer being extremely high. The neutron reaction with the boron gives alpha particles which are much more effective at producing damage than neutrons themselves. A very high rate of damage might be expected under the circumstances. There is insufficient data to comment further on this point.

1.4 SUMMARY

There is wide variation in the sensitivity of the devices examined to neutron radiation, generally because of differences in resistivity of the starting materials and in the importance of lifetime to the device characteristics. The effects of neutrons on body lifetime and resistivity seem to manifest themselves about as one would expect from other measurements. Changes in alpha and junction capacity can be reasonably well accounted for on this basis. However, surface effects do seem to play a very important role in changes in reverse current, and the mechanism is entirely unknown.

There are clearly some gaps in the present experiments that should be filled. The re-etching of germanium transistors and, less important, of silicon diodes to see if one can recover junction currents needs to be done. The silicon devices need to be examined at lower integrated neutron fluxes to see the onset of the lifetime deterioration.

It would be interesting to measure the characteristics in pile and immediately after removal with the hope of observing the changes in surface chemistry that must occur. Different encapsulating environments and containers might show radically different surface sensitivity.

Chapter 2

NOISE AND RELIABILITY OF DIFFUSED SILICON RECTIFIERS

By C. H. Knowles

2.1 INTRODUCTION

For some time the belief has existed that there is a direct correlation between noise and reliability of silicon rectifiers. If this were so, and the correlation could be discovered, then one would have a powerful tool for studying, and possibly predicting, reliability in diffused silicon devices.

The limited study reported herein was undertaken to determine noise characteristics of diffused silicon diodes. Reliability as reflected in 20 hours of aging was measured as a function of noise under various bias conditions in an attempt to find a correlation. The bias conditions were constant-voltage reverse bias, constant reverse current, and constant forward current.

During the measurements, a well-defined relationship was discovered between 1/f noise current and reverse current. That relationship is given in this chapter; further work is anticipated here, however, and will be reported later in more detail.

2.2 DISCUSSION

2.2.1 Noise and Reliability Correlation

Certain types of noise have frequently been associated with surface conditions.*† In particular, 1/f noise has been correlated with reverse "saturation" current. There have also been correlations of noise and short-term drift with reliability in germanium devices.‡§ These have been empirical studies.

We have speculated on the possible correlation of reliability with shaky reverse characteristics.* That is, it might be feared that a diode with a shaky reverse characteristic would develop a low voltage breakdown (V_B) during or after its "shaking."

*G. L. Pearson, H. C. Montgomery, and W. H. Feldman, Journal of Applied Physics, Vol. 27, 1955, pp. 91-92.
†W. H. Fonger, "Transistor One," RCA Laboratories, p. 239 and following.
‡J. H. Forster, personal communication.
§P. Zuk, personal communication.

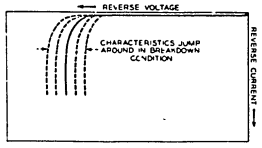

Fig. 1 - "Shakiness" in breakdown

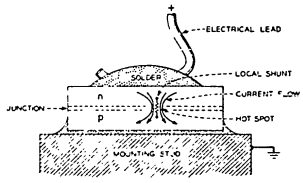

Fig 2 - Proposed mechanism of failure

The mechanism of failure might be described as follows: if a "shaking" diode were in a high-voltage rectifying circuit and developed a low V_B, it might be expected to pass a current limited only by the circuit impedance. Moderate currents (say, 0.1 ampere) at high voltages (say, 100 volts) mean rather high powers (10 watts in the parenthetical case). The power dissipation in this case would probably be highly local, causing high local heating (see Fig. 2). The heat would probably accelerate the mechanism of low V_B, causing further degradation of over-all rectifier characteristics.

We have no theory to present which describes the noise, or shaking, in even a qualitative way. It is, however, observed somewhat as shown in Fig. 1.

2.2.2 Philosophy of Measurements

Noise was measured under three conditions: (1) constant low-voltage reverse bias, (2) constant reverse current, and (3) constant forward current.

Low-voltage reverse-bias noise is measured as in Fig. 3. In this circuit a constant voltage is applied to the diode and the noisy current fluctuations are measured. In this way every diode can be measured in an equivalent fashion, i.e., a given voltage is applied to every diode.

For the case of constant low voltage one expects a shot noise of $\overline{i^2} = 2qI\Delta f$ where $\overline{i^2}$ is the mean square noise current, q is electronic charge, I is the temperature limited current, and Δf is the band width over which $\overline{i^2}$ is measured. The shot noise is seen to be "white"; that is, constant in frequency.

Empirically, many workers in the semiconductor diode field have found a 1/f noise which is superimposed on the shot noise. At low frequencies the 1/f noise

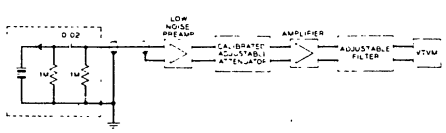

Fig 3 - Noise-measuring circuit, set to measure noise currents at constant reverse voltage

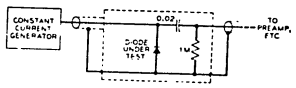

Fig. 4 - Noise current for constant-current measurements

predominates. At high frequencies the shot noise is the noise that is seen. It has been shown experimentally, for germanium, that 1/f noise is proportional to reverse saturation current in some diodes.*

We discovered that, in silicon diodes, there is also a definite correlation between reverse "saturation" current and 1/f noise. The reverse "saturation" current here is due, in all probability to surface leakage, since the currents we observe are much larger than one can predict from the semiconductor body properties. The relationship between noise and reverse current is approximately:

$$i_{rms} = 10^{-4} I_r \frac{\sqrt{\Delta f}}{\sqrt{f}}$$

where i_{rms} is the magnitude of the 1/f noise current when measured at a frequency f and over a bandwidth of Δf, and I_r is the reverse "saturation," or leakage current.

Since the reverse "saturation" currents observed in silicon diodes are probably due to surface conditions, one might expect some correlation between poor reliability (caused presumably by adverse surface conditions) and saturation current. By the relationship noted above, there might also be expected some relationship between low voltage noise and reliability.

We also measured noise voltages under constant-current forward bias. The circuits of Figs. 4 and 5 were used. We measured every diode under constant forward current to get an equivalent measurement for each diode.

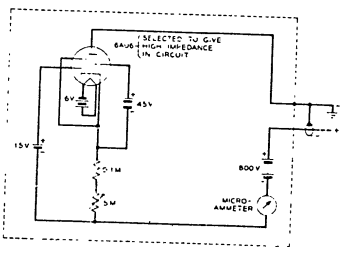

Fig 5 - Constant-current generator

*W. H. Fonger, op. cit.

In the breakdown region, however, we have another matter. The breakdown of which we speak is not the body, or avalanche, breakdown, but is generally conceded to be due to some surface phenomenon. Noise in this region has been little studied. In the region of sloppy voltage breakdown it is difficult to get an equivalent measurement from one diode to the other by using constant voltages. Some diodes have a very high V_B and others very low. Hence, if a measuring voltage which gave meaningful readings in the voltage breakdown of one diode were applied, this voltage might be catastrophically high for poor diodes.

One way of getting equivalent measurements in the breakdown region is to apply a constant current and measure noisy voltage fluctuations. Such a circuit would be as in Fig. 4. The voltage fluctuations pictured in Fig. 1 might be expected to show up with such a circuit.

2.3 MEASURING EQUIPMENT

2.3.1 Noise Spectrometer

The circuit shown in Fig. 3 was used to measure noise. The equipment was made available by H. C. Montgomery, who designed it. The system is fairly free of noise, as may be attested by the fact that we can quite accurately (±0.5 db) measure the noise in a 0.5-megohm resistor. We measured in the frequency range from 30 to 10,000 cps. Figure 7 shows an example of the consistency and the magnitude of the noise measurements.

2.3.2 Constant-Current Generator

The constant-current generator that was developed for use in this circuit is shown in Fig. 5. This circuit is admirably suited for low-noise constant currents from 0.5 μa to 1000 μa. The voltage range over which the circuit will yield constant currents is from zero to 700 volts. The source impedance of this circuit is about 1000 megohms at the low current range and about 100 megohms at the upper current range. It is entirely battery operated and is well shielded, being enclosed entirely in an aluminum box with connection to the noise measuring circuit by shielded cable.

2.4 DIODE NOISE CHARACTERISTICS

Figure 6 shows the noise current spectrum one might expect from a diode under constant reverse-voltage bias. In addition to the diode shot noise, there is shown a 1/f noise. The 1/f noise is predominant at low frequencies. The noise of the diode is shown to be superimposed on the noise of the input resistance of the amplifier. The amplifier is assumed to have zero noise.

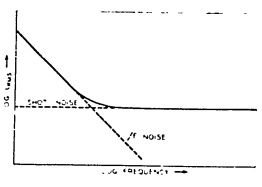

Fig 6 - Expected diode noise spectrum, showing addition of 1/f noise to shot noise

Figure 7 shows the noise spectrum of an M2045 miniature power rectifier with particularly high 1/f noise. It may be seen from Fig. 7 that the noise measurements are quite good, i.e., within about 1 db/cycle at frequencies of 80 cycles and above. For example, one can get a good measurement of the noise in the 0.5-megohm input resistor. The data in Fig. 7 show that for this particular diode 1/f noise predominates out to about 3 kc. This was a rather noisy unit, however, and should not be construed as average. The equivalent Western Electric Company diodes, GA52937, had very low 1/f noise. In fact, the diode noise was masked by the noise of the 0.5-megohm resistor in all but a few units. Therefore, in order to obtain a measurement of the noise under reverse-voltage bias, we were forced to use our noise — reverse-current relationship (Section 3.2.2). Thus, instead of measuring reliability versus noise at reverse-voltage bias, we measured reliability versus reverse current under reverse-voltage bias.

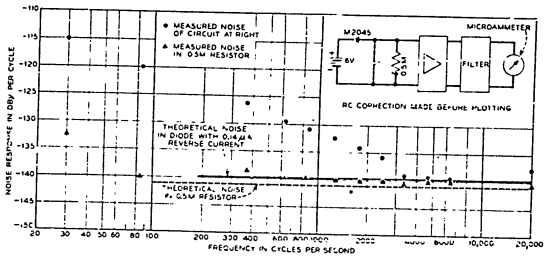

Fig. 7 - Noise spectrum of a very noisy M2045 transistor under -6.0 volts bias

The noise under reverse-current conditions and under forward-current conditions was also observed. Attempts to correlate reliability with these were made.

2.5 MEASUREMENTS OF RELIABILITY

We chose to observe reliability of a large group of GA52937 rectifiers as reflected by a change in voltage breakdown during a 20-hour aging. The short time of aging was dictated by the need for a short-term test which could be used as a manufacturing limit. The noise measurements were interposed just before the standard 20-hour power-aging cycle. The power aging on the rectifiers is done by having each unit rectify 50 ma d-c average current from a 141-volt (rms) source. The voltage breakdown, V_B (that is, the reverse voltage at which the diode conducts -1 μa), was measured before and after aging. The difference in V_B, both positive and negative, was recorded as ΔV_B.

Thus for each diode we have a measurement of ΔV_B, noise at constant reverse current (-1 μa), noise at constant forward current (+1 μa), and reverse current at a constant voltage (-6 v). We can, therefore, plot reliability as reflected by a change in voltage breakdown as a function of three things: noise at a reverse current, noise at a forward current, and "saturation" or leakage current.

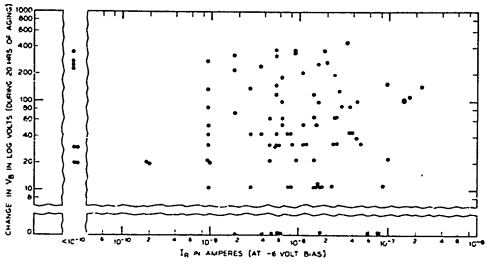

Fig. 8 - Change in V_B versus reverse current

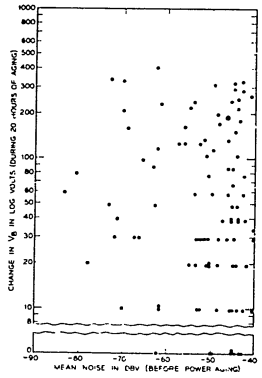

Fig 9 - Change in V_B versus mean noise at -1.0 μa reverse-current bias

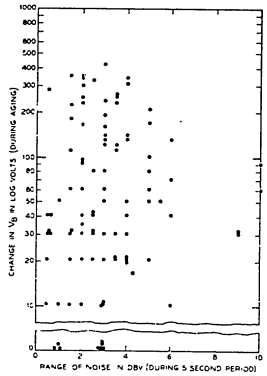

Fig 10 - Change in V_B during aging versus range of noise, with diode under 1 0 μa reverse-current bias

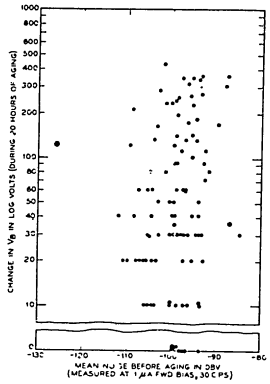

Fig. 11 - Change in V_B versus mean noise at constant-current forward bias

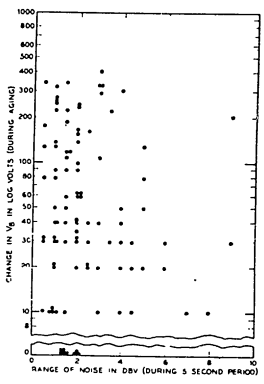

Fig 12 - Change in V_B versus range in noise with diode under 1 0 μa forward-current bias

2.6 RESULTS

The results of the measurements, in brief, showed a complete lack of any correlation between noise and overnight aging. The data are presented in Figs. 8 through 12. Figure 8 shows a plot of ΔV_B, the change in breakdown during overnight aging versus saturation current (i.e., 1/f noise current at a constant reverse voltage). Figure 9 plots ΔV_B versus mean noise in a 5-second period, while the diode was conducting 1 μa reverse current. Figure 10 plots ΔV_B versus the extremes in noise measured during a 5-second period. The extremes in noise are shown here in an attempt to indicate "shakiness" in diode reverse characteristics. The extremes mean little quantitatively without an analysis of the speed of response of the entire measuring system; such an analysis has not been done. Figure 11 shows ΔV_B versus mean noise in a 5-second period with the diode was conducting 1 μa forward current. Figure 12 shows ΔV_B versus the extremes in noise read during a 5-second period.

Figures 8 through 12 give the reader a good idea of the magnitudes and spreads in noise that we observed. They do not, however, indicate any correlation between the measured noise and the measured reliability.

2.7 CONCLUSIONS

There seems to be no correlation between noise and degradation in voltage breakdown during overnight aging of diffused silicon power rectifiers. It is possible that the observed degradation is so large as to mask the correlation between noise and more subtle changes in breakdown that might be expected.

Chapter 3

TEMPERATURE DEPENDENCE OF THE M2039 TRANSISTOR

By J. Sevick

3.1 INTRODUCTION

The M2039 diffused-base germanium transistor is presently designed to function as an oscillator at 200 mc, with an output of more than 50 mw with 200 mw d-c input power. This objective was based upon operation in the neighborhood of room temperature. A very interesting and important question is how these high-frequency germanium transistors operate at elevated temperatures. The answer to this question no doubt will supply valuable information to circuit designers who need the efficiency and high frequency performance of the germanium transistor operating at such elevated temperatures.

High-temperature operation of the M2039 transistor was measured by making performance, high and low frequency, and I_{co} measurements at elevated temperatures on ten units. A simple oven was designed so that existing gear could be utilized while the transistor itself was maintained at a known, elevated temperature. Details of this system are described in Section 3.2. The results of this investigation are then given in the ensuing sections, followed by a summary at the end of the chapter.

3.2 METHOD

Raising the temperature of the transistor was accomplished by exposing the unit to a stream of heated, dry nitrogen. This was made possible through the use of a portable heater, shown in Fig. 13. The orifice of the heating apparatus, through suitable clamping, was made to enclose transistors under all tests whether they were mounted vertically in a rack or horizontally in a jig on the bench. Dry nitrogen, under a few pounds of pressure, was passed over a heated coil of nichrome wire. The heated nitrogen then flowed through an orifice with a diameter of about twice that of the transistor. In a matter of a few minutes, the temperature of the complete system, including the transistor under test, reached an equilibrium value. Temperatures were raised or lowered by varying the current to the nichrome coil. A calibration of the thermometer readings with those of a thermocouple fastened to the header of the transistor showed that deviations were less than a few tenths of a degree centigrade. This was done under bias conditions in order to take into account the added heating effect within the transistor.

This technique of heating not only makes use of existing test gear, but also possesses the advantage of eliminating temperature effects in the external circuitry.

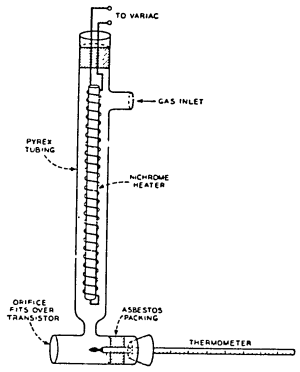

Fig. 13 - Portable heating apparatus

3.3 HIGH-FREQUENCY OSCILLATOR PERFORMANCE

Since the M2039 transistor was primarily designed as an oscillator at high frequencies, oscillator efficiency at elevated temperature was measured first. This was done at three temperatures, 25°C, 60°C, and 100°C, with a constant d-c input power of 200 mw. It was found in all cases that the efficiency went down with increased temperature. The efficiencies of the ten units, together with the median value, are plotted against temperature in Fig. 14.

It is important to note that the transistors oscillated very satisfactorily at 100°C and that all of them remained better than 25 per cent efficient at this temperature. This figure of 25 per cent, which results in 50 mw of output power with 200 mw input, was set as the lower limit of acceptance at room temperatures in the original design of the unit.

In these measurements, the oscillators were adjusted for approximately maximum efficiency at room temperature. No retuning of any kind was done during the temperature run. Presumably, adjustment for best efficiency at 100°C would yield better results at this temperature and flatten the efficiency versus temperature curve somewhat.

3.4 HIGH-FREQUENCY MEASUREMENTS

The alpha cutoff frequency of a transistor can be obtained by common-emitter gain measurement.* This is done by measuring common-emitter short-circuit current gain at a frequency two or more times the common-emitter cutoff frequency

*This work was presented by D. E. Thomas at the Electronics Device Conference, June 1955.

(3-db point) and plotting the result on log-gain versus log-frequency coordinates. A line with a negative 6 db/octave slope is drawn through this point. The intersection of this line and the zero gain line is approximately 80 per cent of the alpha cutoff frequency.

For the ten transistors under investigation, only two temperatures were used in the common-emitter gain measurements. They were 25°C and 85°C. The reason 85°C was used rather than 100°C was that at around 100°C three of the transistors broke into sustained oscillations of about 380 mc. Later it was found that these units exhibited a low-frequency alpha greater than 1 above 85°C.

Table 3-1

Variation of Alpha Cutoff Frequency with Temperature

Unit No.	F_α in Megacycles		Change in F_α/°C
	At 25°C	At 85°C	
1	490	440	0.17%
2	725	600	0.17%
3	550	515	0.11%
4	535	465	0.22%
5	625	505	0.32%
6	515	470	0.15%
7	445	415	0.11%
8	590	515	0.21%
9	800	715	0.18%
10	290	—	—
Average*	583	516	0.18%

*The average value is taken over the first nine units.

Table 3-1 shows the values of the alpha cutoff frequency at the two temperatures and the percentage rate of change of alpha cutoff with temperature. This percentage figure is determined by calculating the change in the alpha cutoff frequency by the method described above and then dividing by the temperature difference. It is interesting to note that five of the units still had, at 85°C, alpha cutoff frequencies greater than 500 mc.

The base resistance of five of the units was measured as a function of temperature. The reason for only using five units was that no significant change in r_b' was noted with temperature. Only one unit showed a change, and this amounted to a total decrease of 4 ohms at 100°C. This represents a change of 4 ohms in 50 or 0.1 per cent per degree centigrade.

The technique for measuring the base resistance has been previously described in Chapter 6 of the Fourth Interim Report and Chapter 9 of the Fifth Interim Report. In brief, it consists of measuring at 250 mcps the real part of the input impedance between base and emitter with the collector shorted for a-c to the emitter. The expression for this input impedance is

$$Z_{in} = r_b' + \frac{Z_e}{(1 - \alpha)} \qquad (3\text{-}1)$$

where Z_e is the total impedance in the emitter circuit. With improved circuitry, inductance effects in the emitter circuit are minimized as described in Chapter 5 of the Sixth Interim Report) and Z_e takes on the value

$$Z_e \simeq r_e$$

$$\simeq \frac{kT}{qI_e} \qquad (3\text{-}2)$$

The order of magnitude of the change in the second term of equation (3-1) can be calculated. It is immediately apparent from equation (3-2) and from the previous result on the alpha cutoff determination that changes under elevated temperatures of r_e and $(1 - \alpha)$ tend to compensate each other. A calculation, using the average values of F_α from Table 3-1 and extrapolating at 6 db per octave back to 250 mc, yields an increase in the magnitude of $(1 - \alpha)$ by a factor of 1.18 at 60°C change in temperature. The numerator, which is equation (3-2), changes by a factor of 1.2.

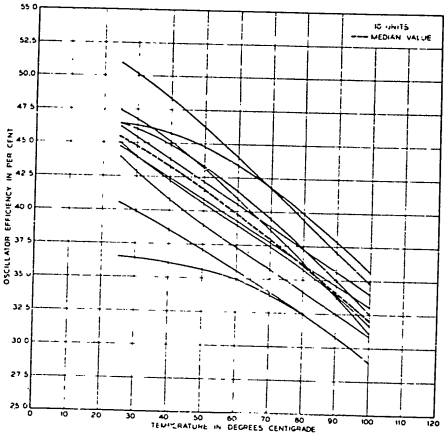

Fig. 14 - Oscillator efficiency as a function of temperature

Therefore, any variation of the input impedance with temperature is mainly dependent upon that of r_b'. The base resistance r_b', in turn, is directly related to the resistivity ρ. Where

$$\rho = (en_o\mu_n + ep_o\mu_p)^{-1} \qquad (3\text{-}3)$$

and n_o = equilibrium electron density

p_o = equilibrium hole density

μ_n = electron mobility

μ_p = hole mobility

e = electronic charge

For the germanium diffused-base p-n-p transistor which has a heavily doped base region, equation (3-3) reduces to

$$\rho = (en_o\mu_n)^{-1} \qquad (3\text{-}4)$$

and n_o is essentially constant over the temperature range. Therefore, it can be assumed from the experimental results that μ_n varies little with temperature. This checks with theory* since at this high level of doping, the mobility is determined mainly by impurity scattering and hence can be constant or increase slightly.

3.5 LOW FREQUENCY h PARAMETERS AND I_{co}

3.5.1 Parameter $1 + h_{21}$

The effect on $1 + h_{21}$, or $1 - \alpha_o$, was an interesting one. All ten transistors showed an increasing α_o with temperature, as exhibited by Fig. 15. The value of α_o can be obtained from the graph by taking the difference between the ordinate value and 1. Three of the units displayed low frequency alphas greater than unity beyond 85 C. Two contributing causes are:

(1) The injection, at the higher temperature, of electrons into the base from the collector, due to the increased electron density in the collector body.

(2) Increase of minority carrier lifetime in the base region with temperature.

*W. Shockley, "Electrons and Holes in Semiconductors" (Princeton, N.J.: D. VanNostrand Company 1955) pp. 286-288.

The first cause stated above is the same as collector multiplication which is found in grown junction transistors.

3.5.2 Input Impedance, h_{11}

The input impedance for the common-base circuit is

$$h_{11} = r_e + (1 - \alpha_o)r_b' = \frac{kT}{qI_e} + (1 - \alpha_o)r_b' . \qquad (3\text{-}5)$$

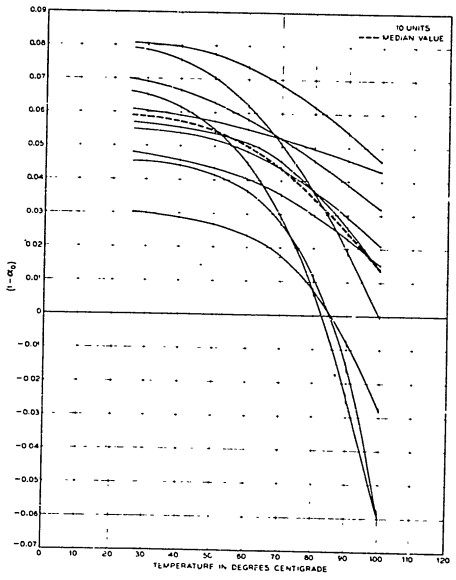

Fig. 15 - $(1 - \alpha_o)$ as a function of temperature

Since r_b' is constant, r_e increasing, and $(1 - \alpha_c)$ decreasing with temperature, it was not difficult to rationalize the data which showed that some of the transistor h_{11} measurements increased slightly while others decreased slightly in going from room temperature to 100°C. In any event, the changes were slight and were not worth plotting.

3.5.3 Voltage Feedback Ratio, h_{12}

The voltage feedback ratio is a result of the base resistance and space-charge layer widening.* The equation for this ratio takes the form

$$h_{12} \simeq \frac{kT}{qw} \frac{\partial w}{\partial V_c} + r_b' h_{22} \qquad (3\text{-}6)$$

where w is the base-layer thickness. This result was verified experimentally, since all ten units showed increasing values of h_{12} with temperature. The median value changed from 1.3×10^{-3} at 25°C to 2.05×10^{-3} at 100°C.

3.5.4 Collector Conductance, h_{22}

The collector conductance can be written as*

$$h_{22} \simeq \frac{kT}{q} \frac{1}{w} \frac{\partial w}{\partial V_c} I_c [2(1 - \beta) + (1 - \gamma)]$$

$$\simeq \frac{I}{w} \frac{\partial w}{\partial V_c} I_c (1 - \alpha_o) + \frac{\partial I_{co}}{\partial V_c} \qquad (3\text{-}7)$$

Experimentally, all units changed very little up to about 70°C. From 70°C to 100°C, most of the units increased in h_{22} by a factor of about 2. Since $(1 - \alpha_o)$ decreased with temperature, $\partial I_{co}/\partial V_c$ increased with temperature. Beyond 70°C, $\partial I_{co}/\partial V_c$ became the dominant term.

3.5.5 Collector Reverse Current, I_{co}

The collector reverse current with 18 volts of collector bias was measured as a function of temperature. The results are plotted in Fig. 16. The median value increased 2.7 microamperes at 25°C to 130 microamperes at 100°C. In an oscillator circuit, for which the M2039 was originally designed, the larger value at 100°C is still only about 1 per cent of the total collector current.

*J. M. Early, The Bell System Technical Journal, Vol. 32, November 1953, pp. 1271-1312.

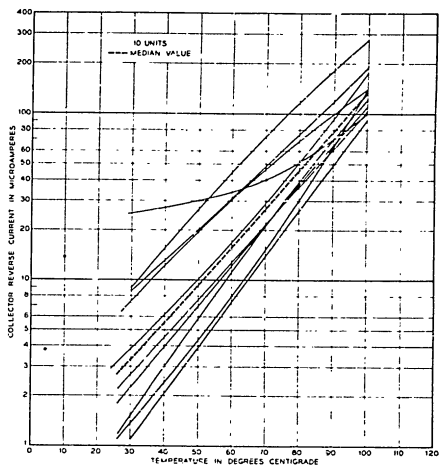

Fig. 16 - Collector reverse current at $V_c = 18$ volts as a function of temperature

3.6 SUMMARY

All ten of the M2039 diffused-base germanium transistors functioned very satisfactorily at elevated temperatures. Indications are that the temperature range can be extended even further.

Oscillator efficiencies dropped only about 12 per cent in going from room temperature to 100°C. The reason for this drop in oscillator efficiency was the reduction in the alpha cutoff at the elevated temperatures. However, six of the units still had, at 85°C, alpha cutoffs equal to or greater than 500 mcps. Small changes occurred with temperature on base resistance, h_{11}, h_{22}, and h_{12}. Low-frequency alphas all went up with temperature. Three units had alphas greater than unity beyond 85°C. I_{co} increased by a factor of about 50.*

By taking into account, the increased collector saturation current and the tendency for some units to have alphas near or greater than 1 at elevated temperatures, diffused-base germanium transistors, with proper circuitries, should give good performance above room temperatures.

Chapter 4

M2055 AND M2058 TRANSISTORS

By J. Sevick

4.1 INTRODUCTION

Considerable progress has been made in development of the M2055 and M2058 low-level high-performance r-f and i-f amplifier transistors during this contract interval. (Development objectives for these units are described in Chapter 8 of the Fourth Interim Report particularly in Table 8-1.) Units are now being fabricated in quantities sufficient for proper evaluation.

Improvements made in the fabrication and measurement of these units, and a preliminary evaluation of these designs are discussed in this chapter.

4.2 FABRICATION PROCESS

A major improvement took place during this report period in the fabrication of the M2055 and M2058 transistors. This was a direct result of the increased effort which was placed on proper tooling. Prior to this period the model fabrication facilities had been largely devoted to the M2039 oscillator unit, of which a large number were made, as reported in Chapter 9 of the Sixth Interim Report. M2058 and M2055 transistors fabricated during that report interval were essentially improvised from the existing M2039 header and tooling. The reason for good progress during the present period is two-fold: (1) a header is being used which is designed particularly for the M2055 and M2058 transistors, and (2) a new cantilever point structure is being employed. Figure 17 shows the new structure of the units.

Previous fabrication attempts consisted of bending one of the insulated leads of an M2039 header, mounting a germanium wafer on a flattened section of this bent lead, and then welding to the sides of the two remaining vertical leads nickel sleeves which contained the balanced C-spring. This process was a natural result of the initial design of the unit, as first described in the Fourth Interim Report. But this process was very difficult to control. Angles on the bent lead were difficult to maintain. Welding to the side of a vertical lead made it practically impossible to keep a point on the small 1- by 2-mil, half-moon, evaporated stripe. The balanced C-springs not only tended to short to each other, but made it very difficult to see if the points were being placed properly.

With a new header and a cantilever construction in the point assembly, much of the original difficulty has been removed. A "spade" is now welded to the insulated

Fig. 17 - Improved structure of the M2055 and M2058 diffused-base transistor

collector lead. Its orientation is quite accurately maintained. Posts with accurately controlled heights form the foundation for the cantilever structure. This new structure, in turn, gives a better view for the placing of the points on the stripes. Finally, by welding the cantilever structure on top of the posts, the tendency for the points to slip off the stripes is greatly lessened.

4.3 ELECTRICAL MEASUREMENTS

All test gear has now been modified in order to accommodate the M2039, M2055, and M2058 transistors. This was made possible largely through the use of a specially designed five-pin socket. Two pins of the socket, the base and the collector, are common to all three transistors. The other three, which are the emitter pins, are then positioned to accommodate the respective transistor.

The only difficulty which was encountered in measuring the M2055 and M2058 transistors appeared in the common-emitter gain measurements at low emitter currents. A gain-versus-frequency curve displayed the standing-wave pattern of an unmatched transmission line. Considerable improvement in accuracy was obtained by increased padding in the transmission lines from the common-emitter gain jig to the mixer, and from the local oscillator to the mixer. A wideband amplifier, using an M2058 transistor, was incorporated in the system in order to increase the output of the test jig. This was found necessary when measurements were attempted at emitter bias currents of less than 0.5 milliampere.

A preliminary study of the data obtained on sixty units indicates that the initial electrical parameters as set forth in the Fourth Interim Report should be realized.

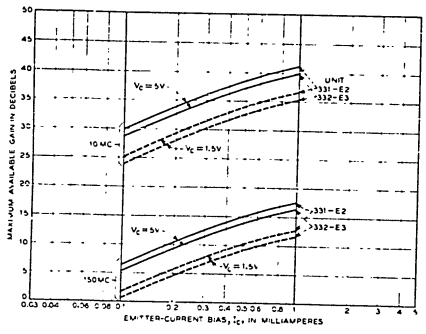

Fig. 18 - Maximum available gain characteristics with bias and frequency for M2055 transistors

Of these units, 60 per cent had common-emitter short-circuit gains, at 100 mc, in excess of 12 db; 33 per cent had gains greater than 14 db. All of the other electrical parameters were in order, with the possible exception of $1 + h_{21}$. The median value presently centers around 0.05, while the objective value is ~0.02. Attention will be given to improving this parameter.

Circuit groups now have these transistors in sufficient quantities in order to evaluate them properly. A plot, by one of the groups, of the maximum available gain as a function of frequency and biases is shown in Fig. 18. The best and the poorest of five units under test are shown in the figure. Initial results in high-frequency amplifier circuits suggest that the theoretical curves of Fig. 18, which are based upon data taken from parameter measurements, are a measure of what is expected from these high-performance r-f and i-f transistors.

4.4 SUMMARY

Particular advances have been made in the fabrication of the M2055 and M2058 transistors. This has been the result of using a new header with cantilever points.

The usual electrical parameter tests are now being made on the M2055 and M2058 transistors. A specially designed five-pin socket modified most of the M2039 test gear for the new units. A wideband amplifier using an M2058 transistor will be incorporated in the common-emitter gain measurement in order to improve the sensitivity.

The measured electrical parameters of sixty units were all within the design objectives, with the exception of $1 + h_{21}$ (i.e., the alpha defect, $1 - \alpha$), whose median value presently is about 0.05. The objective value is ~0.02. Attention will be placed here.

Chapter 5

STATUS OF THE M2036 P-N-I-P SILICON POWER TRANSISTOR

By J. T. Nelson and J. E. Iwersen

5.1 INTRODUCTION

In the previous discussion of the development of the M2036 5-watt, 10-mc silicon intrinsic-barrier transistor (in the Sixth Interim Report), we reported on the measurements of several parameters and on the oscillator performance of the first units. At the time, these numbers were not up to design objectives and several improvements in the structure were suggested which would bring the values to the desired levels. This report gives the results of carrying out the improvements and shows the progress made toward more complete characterization.

5.2 CHANGES IN STRUCTURE AND ROUGH RESULTS

The structural changes proposed in the last report were (1) to diminish the area occupied by the emitter, the base contacts, and the space between, in order to lessen the base resistance and collector capacitance; (2) to make the base thinner to increase the alpha cutoff frequency (and, incidentally, the low-frequency alpha); and (3) to increase the base-layer doping to reduce the base resistance.

Figure 19 shows the approximate present structure. Most of the recommendations have been carried out. Steps (1) and (2) have decreased the collector capacitance by a factor of three and increased the alpha cut off by a factor of from two to three. Since (2) also tends to increase the base resistance, these procedures have competing effects on this parameter and, in fact, leave it relatively unchanged. In attempting to carry out step (3) we encountered base-to-emitter shorts (possibly because we had a p-n junction degenerate on both sides near the surface). Further work can be done here, but we have backed off at present to concentrate on more pressing matters.

5.3 ELECTRICAL CHARACTERIZATION

5.3.1 Introduction

Since emphasis during this quarter has been placed on structural changes that would improve the performance of the transistor, data have not been accumulated on a large number of units. Because of this, no statistical analysis of parameters is given. The information presented represents typical units and is the result

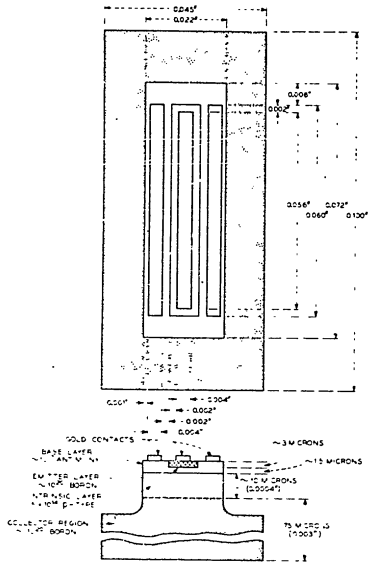

Fig 19 - Revised structure of M2036 transistor
(vertical scale of cross section exaggerated)

of a search for the best method by which to characterize the transistor so as to obtain a correlation between its physical structure and its electrical behavior, and to indicate the degree to which it meets its design objectives. This is necessary to determine defects in the transistor and to bring fabrication processes under control. The characterization indicates that the transistor is capable of meeting its original design objective of delivering 5 watts at 10 megacycles per second and that further improvement could be obtained.

5.3.2 Static Characteristics

The design objectives call for a transistor that will operate with a maximum collector voltage of 100 volts and a maximum collector current of 400 milliamperes (see Chapter 21 of the Thirteenth Interim Report, Second Engineering

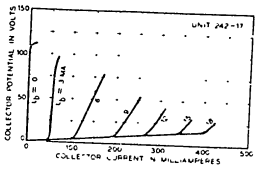

Fig 20 - Common-emitter static characteristics

Services Contract). A minimum voltage no greater than 10 volts at the maximum current is desired. Common-emitter static collector characteristics of the transistor are shown in Fig. 20. Little difficulty is encountered in meeting the maximum voltage requirement. Negligible collector current is drawn with zero base current, out to a breakdown in excess of 100 volts. The high current performance does not quite meet the requirement. There is a falloff of current gain at high current with low collector voltage, as well as a series collector resistance of approximately 40 ohms. Difficulty of control over the intrinsic-layer thickness is at present partially responsible for the series resistance.

5.3.3 Collector Capacitance

Collector capacitance as a function of collector voltage for the revised structure is shown in Fig. 21. The collector capacitance has been reduced by a factor of two from that encountered in the previous structure (see Chapter 11 of the Sixth Interim Report). More careful etching of the collector junction will permit a reduction of from three to four. As in the previous structure, there is no leveling off of the capacitance as the space charge is swept into the collector region, as would be expected with a step junction between the collector and intrinsic layers. Rather, the presence of the diffused collector results in lower slope in the variation of capacitance with voltage than would be present without the collector (n-i junction only).

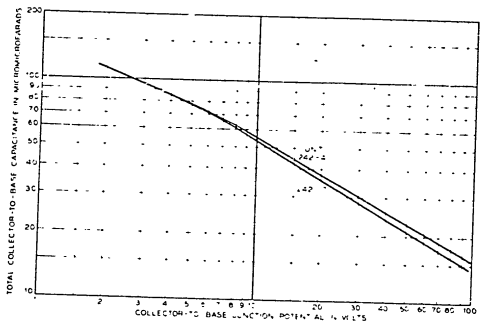

Fig 21 - Collector capacitance as a function of voltage

It should be pointed out that this is the total capacitance between the collector and base. It will be shown later that only about a third of this capacitance limits the amplifier performance of the transistor when used where neutralization is possible.

5.3.4 Small-Signal Current Gain

Figure 22 shows the small-signal common-emitter current gain as a function of collector current. Collector junction voltage was maintained at 30 volts over the current range. The current gain appears to remain high, from 20 milliamperes out to 500 milliamperes, where power dissipation terminated measurements. More recent measurements by pulse techniques tend to indicate small-signal measurements made in this fashion are apt to be misleading because there is a strong dependence of current gain on temperature. Since the current gain increases with temperature, a fall-off of gain with current may be masked by the temperature effect due to greater power dissipation at high current. It will therefore be necessary to investigate variation of current gain with bias current in such a manner that the average power dissipated in the transistor will remain constant.

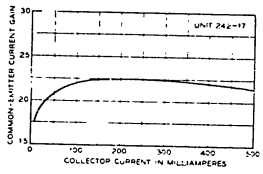

Fig. 22 - Common emitter current gain as a function of collector current

The variation of small-signal common-emitter current gain with frequency is given in Fig. 23. If the grounded base f_α is calculated by the approximate relation $f_\alpha = f$ emitter$/(1 - \alpha_o)$, an f_α of 60 megacycles per second is obtained for transistors

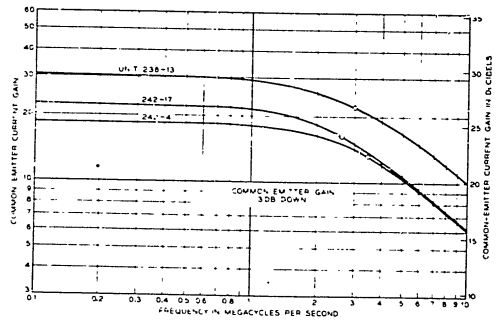

Fig 23 - Common-emitter current gain as a function of frequency

242-4 and 242-17, and an f_α of 90 megacycles per second for 238-13. (The base-layer width is 1.6μ for 242-4 and 242-17 and 1.4μ for 238-13.) The actual common-base f_α is probably in excess of these values.

5.3.5 Proposed Equivalent Circuit and Measurements at 10 Megacycles

Since the transistor will operate at or near 10 megacycles, we desire an accurate characterization at this frequency. Figure 24 shows the proposed equivalent circuit, which is seen to be the usual high-frequency "T" plus an element, C_o, called the outer capacity, to distinguish it from C_i, the inner capacity. $C_o + C_i = C_t$, the total collector capacity, which is the quantity measured by the usual means. We have dotted in a series-collector body resistance (r'_c) in the equivalent circuit, since the static characteristics show that one exists and is of the order of tens of ohms. However, this measurement is made at a few volts and, if r'_c is due to unswept π type material, as seems reasonable, it should decrease with voltage and, in a properly constructed transistor, be negligible at the operating point. In any case it can be treated as part of the termination, so no account of it has been taken in the following.

Without measuring transmission properties, such as transfer impedances, which is difficult, we can still get three independent parameters by measuring the input and output open-circuit impedances (z_{11} and z_{22}) and the input and output short-circuit admittances (y_{11} and y_{22}). The relationship $z_{11}y_{11} = z_{22}y_{22}$ allows a check. These parameters are, neglecting negligible terms:

$$z_{11} = \frac{r'_b + r_e + \frac{C_o}{C_i}[r'_b\ (1 - \alpha) + r_e]}{\frac{C_t}{C_i} + jr'_b\omega C_o} \qquad y_{11} = \frac{1 - \alpha}{r'_b\ (1 - \alpha) + r_e} + j\omega C_o$$

$$z_{22} = \frac{\frac{1 - \alpha}{j\omega C_i} + \frac{C_o}{C_i}[r'_b\ (1 - \alpha) + r_e]}{\frac{C_t}{C_i} + jr'_b\omega C_o} \qquad y_{22} = \frac{(r'_b + r_e)\ j\omega C_i}{r'_b\ (1 - \alpha) + r_e} + j\omega C_o$$

where $\alpha = \dfrac{\alpha_o}{1 + j\dfrac{\omega}{\omega_\alpha}}$

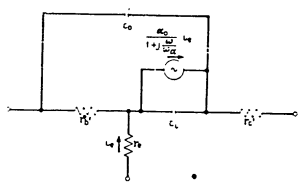

Fig 24 - Proposed equivalent circuit (showing common emitter)

Measurements were performed on unit 242-17. (This unit was selected at random from the first few to meet the 5-watt, 10-megacycle objective, not for any reason having to do with fit to theory.) $kT/qI_e = 0.13$ ohms at room temperature (I_e = 200 milliamps.) but, making allowance for the operating temperature and some small contact and series resistance, we assume $r_e = 0.16$ ohms. C_t is taken from Fig. 21 at the bias point of 30 volts where it equals 28 micromicrofarads. $\omega_\alpha = 391 \times 10^6 sec^{-1}$ and $1 - \alpha_o = 0.0426$ are taken from Fig. 23. The ratio C_t/C_l is estimated equal to 4, from the ratio of the total collector area to the emitter area. (The capacity under the space between emitter and base contacts should be connected to the base contact, since almost all the base resistance occurs under the emitter and very close to it.) Figure 19 gives this ratio as 3.3 but the value 4.0 was measured on the actual transistor. The only parameter fitted to the measurements is r'_b, however, this procedure is fairly direct, since the conductance portion of y_{11} is closely identical to $1/r'_b$. All these numbers, together with $r'_b = 35.5$ ohms, yield:

$$z_{11} = 10.7 + j3.6 \text{ ohms}$$
$$y_{11} = 0.028 + j0.0020 \text{ ohms}^{-1}$$
$$z_{11}y_{11} = 0.292 + j0.127$$
$$z_{22} = 86 - j35 \text{ ohms}$$
$$y_{22} = 0.0024 + j0.0025 \text{ ohms}^{-1}$$
$$z_{22}y_{22} = 0.294 + j0.131$$

Measurements of these four parameters were made on a Boonton R-X meter, using appropriate transmission-line transformers. The measured values are:

$$z_{11} = 10 + j1.5 \text{ ohms}$$
$$y_{11} = 0.028 + j0.002 \text{ ohms}^{-1}$$
$$z_{11}y_{11} = 0.28 + j0.062$$
$$z_{22} = 65 - j25 \text{ ohms}$$
$$y_{22} = 0.0034 + j0.0028 \text{ ohms}^{-1}$$
$$z_{22}y_{22} = 0.29 + j0.10$$

The difference between the products of the measured values ($z_{11}y_{11}$ and $z_{22}y_{22}$) shows that there are inconsistencies in the measured values comparable to the differences between the measured and calculated values. The fit is remarkably good, especially in view of the a priori nature of four of the five components of the equivalent circuit. Error in measurements results from the difficulty in providing bias to the transistor and at the same time providing an a-c open circuit (z_{11} and z_{22}). For the admittance measurements (y_{11} and y_{22}) it is necessary to provide an a-c short circuit which is small compared to the input and output impedances. For example, in the y_{22} measurement the base must be shorted by an impedance small compared to 10 + j1.5 ohms. This could not be done without great difficulty, since the transistor header and socket lead inductance has a reactance of about 1 ohm. In order to obtain closer agreement between the equivalent circuit and the measurements it may become necessary to include the lead inductance in the equivalent

circuit. However, until the inconsistencies in the measured values themselves can be reduced, there is little point to complicating the equivalent circuit.

In spite of the fact that secondary effects such as lead inductance have been neglected, there is such good agreement between the calculated and measured values that we intend to adopt the equivalent circuit of Fig. 24 as representative of the M2036 at radio frequency.

The unilateral power gain calculated from the measured parameters for unit 242-17 gives 95 or 19.8 db at 10 megacycles per second, compared to about 6 or 7.8 db given for transistors reported on in the previous quarter.

5.3.6 Oscillator Performance

An oscillator has been built to see if the M2036 transistor would meet the objective of delivering 5 watts at 10 megacycles per second. The oscillator shown in Fig. 25 has been treated as a common-emitter circuit with a pi feedback network, ($C_3 L_3 C$), between collector and base. The collector is grounded to a heat sink. Power output was determined by measuring the voltage across the load resistor R_3 by means of an oscilloscope. The values of components in the feedback network were estimated so that feedback would be of proper phase and magnitude, using the measured real parts of the input and output impedances and an assumed 90° phase shift from base to collector. The calculated values did not give the best oscillator performance. This might be expected, since the calculations were based on crude assumptions and on small-signal linear measurements, while the oscillator operates over the entire nonlinear range. However, the values were within a factor of two of the optimum and gave oscillation within 25 per cent of 10 megacycles per second. By adjusting the components in operation for maximum output, over 5 watts at 10 megacycles per second was obtained.

Oscillation has been detected at 102 megacycles when the feedback network was reduced to a minimum, i.e., wiring capacitance and lead inductance.

5.3.7 Pulse Measurements of Parameters

Because of the temperature dependence of current gain, it has been found difficult to determine meaningful $\alpha - I_e$ and static curves of the transistor at several

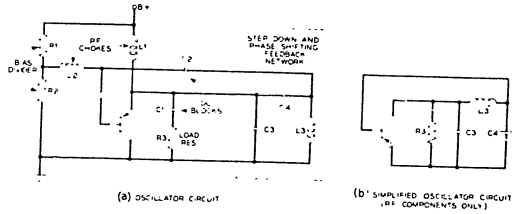

(a) OSCILLATOR CIRCUIT (b) SIMPLIFIED OSCILLATOR CIRCUIT (RF COMPONENTS ONLY)

Fig. 25 - Schematic diagram of oscillator circuit

bias points. Changing the bias point changes the power dissipated within the transistor, which results in a change of temperature and current gain. This effect was mentioned in Section 3.3.2 in connection with the current gain versus collector-current plot. To provide a check on the measurements already taken, and to extend them to high currents, pulse techniques will be used. Preliminary measurements have been made which indicate that this method of attack will be effective.

5.4 SUMMARY AND FUTURE PLANS

Changes in design of the M2036 have been carried out and considerable improvement has been noted in the electrical characteristics. Reduction of the area of the emitter, the space between the emitter and base contacts, and the thickness of the base region have resulted in lowered collector capacitance, increased frequency cut-off of alpha, and increased low-frequency current gain. These changes have also increased the unilateral power gain by better than a factor of 10.

An equivalent circuit has been adopted for the transistor. It is the usual high-frequency "T" with an added outer capacitance between base and collector. The validity of the equivalent circuit was checked by a close agreement between four pole parameters calculated by means of the equivalent circuit with the measured values of the same parameters.

Oscillator performance now indicates the transistor is capable of meeting the design objective of delivering 5 watts at 10 megacycles per second. Measurement of static characteristics by pulse techniques has been found necessary and has been initiated.

During the next interval, pulse techniques will be applied in order to measure transistor parameters at constant temperature. An attempt to reduce the labor in characterization will be carried out. Fabrication processes will be looked into with an eye toward decreasing the collector-body series resistance.

TASK 5 - TRANSISTOR TEST METHODS

Chapter 6

REVIEW OF TASK 5 ACTIVITIES

By H. G. Follingstad and O. Kummer

6.1 INTRODUCTION

Development of the 5-mc to 250-mc Phase Set continued in this period. The set will completely and accurately define transistors in this frequency range, with magnitude and phase of four insertion parameters. The latter are fully discussed in Chapter 8 of the Second Interim Report. Design objectives and a functional description of the 5-mc to 250-mc Phase Set were presented in Chapter 11 of the Fourth and Chapter 12 of the Sixth Interim Report. This chapter outlines the present status of development of the set in terms of the block functions of Fig. 26.

6.2 MEASURING-PATH SWITCHES

Measurements on the transfer switch described in Chapter 14 of the Sixth Interim Report indicate crosstalk between standard and unknown path to be 37 db at 100 mc. The switch has been redesigned and tests on a prototype model indicate crosstalk between standard and unknown to be lower than 70 db.

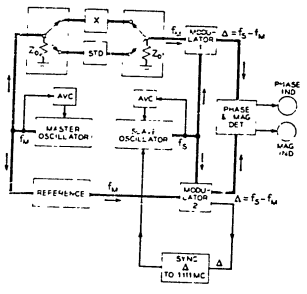

Fig. 26 - Block diagram of the 5-mc to 250-mc phase set

6.3 AMPLIFIER MODULATOR NOISE TESTS

Over-all measurements on the noise level in the set indicate a signal-to-noise ratio of 20 db when the signal is at the lowest operating level of -80 dbm. Tests on the amplitude indicator show that an error of about 0.1 db is produced by noise when the signal is 20 db above noise. This should correspond to an error no greater than 0.6 degree in the phase indication.

6.4 SYNCHRONIZATION

In the process of testing the 5-mc to 50-mc servo and electronic loops, the system performance was improved by the following means:

(1) Reduction in mechanical friction at the slave-oscillator control shaft.

(2) Increased slave-oscillator output in the presence of transistor network loading.

(3) A monitoring circuit to accurately measure deviation of i-f frequency from synchronism and to tune the discriminator.

(4) Greater signal-to-noise ratio in the loop.

Important advantages in reliability of operation are expected by the use of an improved scanning technique which features independence of scanning speed from servo loop gain, elimination of false synchronizing frequencies, and elimination of discriminator offset tuning formerly required for scanning purposes.

SECTION 5 - CONCLUSIONS

TASK 2 - TRANSISTOR RELIABILITY

While a continuation of the direct determination of aging behavior continues to be essential it is also of the greatest importance to get a better understanding of the physics of the processes. From the failure of the attempt to correlate noise with aging, it is concluded, not that there is no correlation, but rather that the noise currents and aging rates depend on a complex of factors which need to be better understood before any such correlation will be evident. Work in progress toward such objectives is mentioned in Section 6.

TASK 4 - NEW AND IMPROVED TRANSMISSION-TYPE TRANSISTORS

Temperature studies of the M2039 diffused-base p-n-p germanium oscillator design have shown that 200-mc oscillator output power is decreased about a fourth by increase of the operating temperature from 26°C to 100°C. Direct-current, low-frequency, and high-frequency parameters were shown to vary in approximately the way expected from theory. Measurements of initial models of the M2055 and M2058 low-level germanium diffused-base amplifier transistors indicate that these designs will be satisfactory. This diffused-base germanium work under Industrial Preparedness Contract DA 36-039 sc-72729 will continue.

The high-power performance capability of the M2036 diffused-base 5-watt 10-mc p-n-i-p silicon transistor has been demonstrated. Initial characterization studies indicate a satisfactory equivalent circuit can be developed. The improvements in performance to give better than 5 watts r-f output at 10 mc are attributed almost entirely to the modifications in design instituted during the contract interval.

TASK 5 - TRANSISTOR TEST METHODS

The present status of the 5-mc to 250-mc Transistor Phase Set has been outlined; development and prove-in of the brassboard model will continue.

SECTION 6 - PROGRAM FOR NEXT INTERVAL

TASK 2 - TRANSISTOR RELIABILITY

The direct determination of aging rates continues, since it is needed to predict reliability in systems, particularly for the newer transistors. Among the tests is one to separate temperature dependence and voltage dependence of aging rates. Statistical procedures for the improvement of efficiency of data are being developed.

Attempts to correlate junction characteristics with surface properties, such as surface potential and recombination velocity, are being made.

TASK 4 - NEW AND IMPROVED TRANSMISSION-TYPE TRANSISTORS

Industrial Preparedness Study Contract work on diffused-base germanium transistors will be concentrated on the M2039 oscillator transistor mechanical structure and on the M2055 and M2058 low-level amplifier designs. Characterization of the latter devices will be emphasized, with particular concentration on the high-frequency performance. Noise and linearity studies will also be reported.

M2036 diffused-base 5-watt 10-mc silicon transistor work under Task 4 will include use of pulse techniques in order to measure transistor parameters at constant temperature. Efforts will be made to simplify characterization techniques. Modifications of fabrication processes in order to decrease collector body series resistance will be undertaken.

TASK 5 - TRANSISTOR TEST METHODS

Testing of the Phase and Magnitude Indicator as a unit will be completed. The synchronization function will be proved in using an improved flexible scanning technique. Design of range switching and standard-unknown path switching panels will be completed.

Construction of the prototype will be started by Stavid Corporation, according to information obtained from the brassboard model.

SECTION 7 - IDENTIFICATION OF PERSONNEL

Preceding reports under this contract have identified the engineers and scientists whose work has contributed materially to the progress of the studies and investigations conducted during the periods covered by the reports. During the current period, additional personnel were assigned to work on portions of this contract. Brief biographies of these individuals are provided below.

WALTER L. BROWN

Walter L. Brown received his B.S. from Duke University in 1945, his M.A. in 1947, and his Ph D. in Physics in 1951 from Harvard University. He joined the Laboratories in 1950. His principal interest at the Laboratories has been in the study of surface states on germanium and silicon surfaces and in the effects of radiation, primarily high-energy electrons, in introducing imperfections in the structure of these two semiconductors. His current work is directed toward understanding the significant mechanisms in the simplest type of radiation damage, namely that introduced by bombarding particles whose energies are close to the threshold for the damage process.

CARL HARRY KNOWLES

Carl Harry Knowles was born in Birmingham, Alabama, in 1928. He was in the United States Marine Corps from 1946 to 1948. He received a B.S. in Physics from Alabama Polytechnic Institute (Auburn) in 1951, and an M.S. in Physics from Vanderbilt University in 1953.

Mr. Knowles has been employed at Bell Telephone Laboratories since leaving Vanderbilt, and he completed the BTL Communications Development Training Program in 1956. During his employment at the Laboratories, Mr. Knowles has been employed in semiconductor device development.

JERRY SEVICK

Jerry Sevick received his B.S. in Education from Wayne University in 1940. From 1942 to 1945 he was in the U. S. Army Air Force. During his service he completed pilot training in Texas and radar training at Harvard and M.I.T. At the time of discharge, he was a project director for radar devices at Wright Field. In 1946 he went back to Wayne University and obtained an M.S. in Physics. After three

years of teaching at Wayne University, he returned to Harvard University for graduate training. Mr. Sevick received his Ph.D. in Applied Physics in 1952 for a study in the application of the variational technique to problems in electromagnetic scattering by coupled objects.

After three more years of teaching at Wayne University and consultant work in Detroit industry, Mr. Sevick joined the Bell Telephone Laboratories. At the present time he is a member of the Device Development Department, assigned to the Transistor Development Group.

During the period covered by this report, 16 June through 15 September 1956, approximately 5,000 man hours were devoted by key personnel to work on this project.

DISTRIBUTION LIST

150 copies to: Transportation Officer, Signal Corps Engineering Laboratories
Evans Signal Laboratory, Building 42
Belmar, New Jersey
Marked For SCEL Accountable Officer (Inspect at destination)
File No. 144-PH-55-91(1210)

150 copies to: Department of the Navy
Bureau of Ships, Code 816B
Washington 25, D.C.
Attention: Mr. A. M. Andrus

20 copies to: Commanding General, Wright Air Development Center
Wright-Patterson AFB
Dayton, Ohio
Attention: Mr. R. D. Alberts, WCRET-4

5 copies to: A. J. Busch, Bell Telephone Laboratories

5 copies to R. R. Deutsch, Western Electric Company

2 copies to each of the following:

G. W. Gilman, Bell Telephone Laboratories
L. C. Jarvis, Western Electric Company
A. C. Keller, Bell Telephone Laboratories

1 copy to each of the following:

A. T. David, Western Electric Company
F. P. Lyons, Western Electric Company
H. R. Strobel, Western Electric Company
E. Temple, Western Electric Company
J. E. Tweeddale, Western Electric Company

H. A. Affel, Bell Telephone Laboratories
A. E. Anderson, Bell Telephone Laboratories
A. F. Bennett, Bell Telephone Laboratories
E. A. Bescherer, Bell Telephone Laboratories
A. K. Bohren, Bell Telephone Laboratories
E. B. Cave, Bell Telephone Laboratories
M. H. Cook, Bell Telephone Laboratories
P. S. Darnell, Bell Telephone Laboratories
R. L. Dietzold, Bell Telephone Laboratories
H. T. Friis, Bell Telephone Laboratories
K. E. Gould, Bell Telephone Laboratories
W. H. C. Higgins, Bell Telephone Laboratories
A. G. Jensen, Bell Telephone Laboratories
H. A. Lewis, Bell Telephone Laboratories
W. D. Lewis, Bell Telephone Laboratories
C. A. Lovell, Bell Telephone Laboratories
M. B. McDavitt, Bell Telephone Laboratories
J. F. Molnar, Bell Telephone Laboratories
L. W. Morrison, Bell Telephone Laboratories
J. A. Morton, Bell Telephone Laboratories
F. T. Mottram, Bell Telephone Laboratories
L. G. D. Paterson, Bell Telephone Laboratories
A. J. Pietenpol, Bell Telephone Laboratories
W. T. Pyle, Bell Telephone Laboratories
W. E. Reichle, Bell Telephone Laboratories
V. L. Rosel, Bell Telephone Laboratories
F. J. Singer, Bell Telephone Laboratories
M. Sparks, Bell Telephone Laboratories
A. Tradup, Bell Telephone Laboratories
R. L. Wallace, Bell Telephone Laboratories
J. M. West, Bell Telephone Laboratories
A. H. White, Bell Telephone Laboratories

51 copies to. R. M. Ryder (Project Engineer), Bell Telephone Laboratories